Control of an Asymmetrical Design of a Pneumatically Actuated Ambidextrous Robot Hand

Emre Akyürek, Anthony Huynh, Tatiana Kalganova

Abstract—The Ambidextrous Robot Hand is a robotic device with the purpose to mimic either the gestures of a right or a left hand. The symmetrical behavior of its fingers allows them to bend in one way or another keeping a compliant and anthropomorphic shape. However, in addition to gestures they can reproduce on both sides, an asymmetrical mechanical design with a three tendons routing has been engineered to reduce the number of actuators. As a consequence, control algorithms must be adapted to drive efficiently the ambidextrous fingers from one position to another and to include grasping features. These movements are controlled by pneumatic muscles, which are nonlinear actuators. As their elasticity constantly varies when they are under actuation, the length of pneumatic muscles and the force they provide may differ for a same value of pressurized air. The control algorithms introduced in this paper take both the fingers asymmetrical design and the pneumatic muscles nonlinearity into account to permit an accurate control of the Ambidextrous Robot Hand. The finger motion is achieved by combining a classic PID controller with a phase plane switching control that turns the gain constants into dynamic values. The grasping ability is made possible because of a sliding mode control that makes the fingers adapt to the shape of an object before strengthening their positions.

Keywords—Ambidextrous hand, intelligent algorithms, nonlinear actuators, pneumatic muscles, robotics, sliding control.

I. INTRODUCTION

ON a previous stage of this research, a robot hand had been designed with a unique ambidextrous design, which means fingers can curve in both ways to perform either as a left hand or as a right hand [1]. In addition to reaching a range almost twice larger than human hands or other dexterous robot hands [2], [3], a specific finger tendon routing shown in Fig. 1 has also been engineered to minimize the number of actuators. As it can be seen, the proximal phalange is driven by only one active tendon, "pl", instead of the two antagonist ones that would be used if the ambidextrous model were a symmetrical imitation of more conventional designs, such as the ones described in [4], [5]. The action of the removed tendon "pr" is compensated by pulling the two tendons controlling the medial and distal phalanges "ml" and "mr" together. However, the parallel motion of the three phalanges requires high accurate pulling ratios to avoid the tendons to break and to maintain the whole system stability.
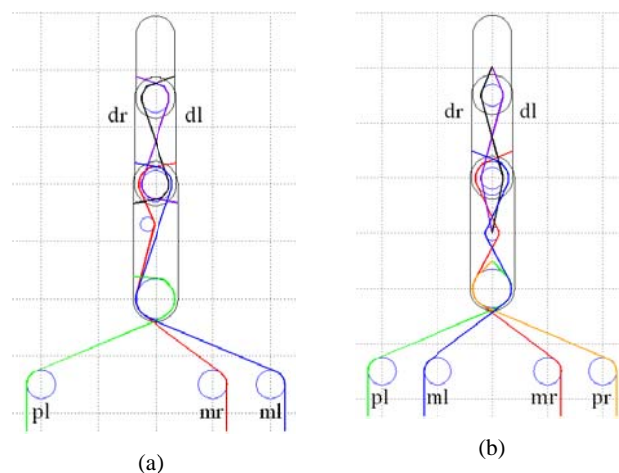
Fig. 1 Finger tendon routings, where "dr" and "dl" are passive tendons assuring a coupled motion between distal and medial phalanges, whereas "pl", "mr", "ml" and "pr" are active tendons linked to actuators that directly control the finger motion (a) is a three tendons routing used for the ambidextrous hand's fingers and (b) is a more classical four tendons designs, also used in previous stages of the project

Besides, the ambidextrous hand is controlled by pneumatic artificial muscles (PAMs), which have a nonlinear behavior [6], meaning their elasticity constantly varies when they are under actuation. Thus, the length of PAMs and the force they provide may differ for a same amount of pressurized air, which causes variations on fingers positions and on their gripping force. Over the past decade, their hysteretic effect could, for instance, be countered interacting directly with the material by radially folding the pneumatic membrane [7]. In this example, the system is then driven using an adaptive PID angle controller combined with two bang-bang pressure controllers. In [8], the force and trajectory tracking control of a PAM actuator are respectively calculated based on the ideal gas equation and on an inverse Laplace transformation of a transfer function. The manipulator described in [9] is controlled based on the anticipation of the parametric nonlinearities that are adaptable to specific movements. The use of a small tracking error allows an additional security to reinforce the projection mapping of the system. The lower-limb introduced in [10] is controlled because of the construction of a hysteresis model, from which the feedforward is compensated with an inverse control.

Thus it is seen that a number of different methods can be used to deal with PAMs' nonlinearity. The Ambidextrous Hand includes Hall Effect sensors and pressure transducers, both joints angles and muscles pressures can be used as data

World Academy of Science, Engineering and Technology
International Journal of Mechanical and Mechatronics Engineering
Vol:8, No:5, 2014

feedback. Given that early designs of ambidextrous fingers were controlled with the parallel form of PID loops [11], a similar layout of algorithms has still been used to control the angular displacements of the final models. Nevertheless, the new asymmetrical design required the use of dynamic gain constants to add more stability around some specific setpoints. These coefficients vary according to the joints position using a phase plane switching control (PPSC) similar to the one described in [12]. Moreover, a further solution was looked for, to add more robustness to the Ambidextrous Robot Hand control algorithms concerning the force applied by the fingertips, and so their grasping features. Previous researches show that SMC is quite frequently used in this area, as it permits to deal with parameters uncertainty [13] by stabilizing the error dynamics of nonlinear mechanisms [14]. In [15], the chattering phenomenon of a robot driven by PAM is reduced with high order sliding mode. SMC has also been combined with neural network to estimate unknown plant dynamics [16]. Finally, as the solid analysis for nonlinear models driven by PAMs described in [17] presents better results for SMC than for flatness-based control and backstepping control, SMC has been investigated to interact with the position features of the Ambidextrous Hand. Once the SMC reaches its objective, a second PPSC puts the system back under the control of PID loops.

To cut a long story short, the developed control algorithms must cover the huge range of the ambidextrous fingers, taking into account both their design asymmetry and the PAMs' nonlinearity. In order to proceed, standard PID loops, dynamic gain constants and SMC continuously relay to each other during finger motion, according to the priority order estimated by two PPSCs. The approach presented in this paper is organized as follows. First, classic PID loops are used to control the ambidextrous fingers asymmetrical design. The weak points of the algorithm are revealed, as well as the implementation of dynamic coefficients when the phalanges must reach critical angles. The evolution of kinematic motion is studied to anticipate the transition of coefficients and to avoid the system becoming unstable. In a second part, a sliding surface is modelled when the fingers get in contact with an object, so the Ambidextrous Hand can properly hug its shape.

II. CONTROL OF ANGULAR DISPLACEMENTS

A. Parallel PID Form Adapted to the Asymmetrical Design

As angular feedback is measured straight from joints, the PAMs nonlinearity does not directly interfere in the control of phalanges displacements. Consequently, the simplest solution consisted in adapting the previous control algorithms to the asymmetrical design. Thus, series of experiments have been performed on ambidextrous fingers, moving them between their extreme positions using small pulses, to bring the phalanges to the desired angles step by step. The pressure feedback of the different PAMs is indicated in Fig. 2, with the fingers extreme positions numbered from 1 to 9. The experiments were done starting from both extremums to the

other, so the hysteretic behavior of PAMs could be averaged. First, it can be seen that the right and left PAMs function in antagonist way, which means the parallel form of a PID controller can be used in a classic way with the equation:

$$u(t) = K_p e(t) + K_i \int_0^t e(\tau)d\tau + K_d \frac{d}{dt}e(t) \qquad (1)$$

and the tuning methods such as explained in [18]. In that case, the correcting output $u(t)$ depends on the error $e(t)$, which corresponds to the difference between the target value and the current data feedback, as well as on the gain constants K_p, K_i and K_d that are respectively the proportional, integrative and derivative constants. When the system is tuned properly, they allow for increasing the fingers' reactivity, sensibility and stability, avoiding overshoots and oscillations. As left and right muscles are antagonist, they vary according to the same amount of pressure (and consequently at the same speed) to make the medial and distal phalanges reach an angular target θ_t. Therefore, the same gain constants are attributed to both of these PAMs, but reacting in opposite ways, which means the first one contracts whenever the second one relaxes. However, it is also noticed in Fig. 2 that the proximal PAM's pressure is often about twice as large as the sum of the two others when the proximal PAM is involved, and so can be its pressure variation from one position to another. This is the reason why starting points and setpoints are compared to each other before any movement. Using an approach similar to the one described in [19], pressure variations are estimated from the data collection, so the ratio is applied to the constant gains of the proximal PAM, which makes it react, more or less, faster. As the sum of pressures for the left and proximal PAMs on the finger's left side corresponds to the sum of pressures for the left and right PAMs on the finger's right side, this provides a kind of symmetry that makes the system possible in most of cases. However, this symmetry deforms itself when the proximal phalange is close to a vertical position. This is why the vertical position must be anticipated to replace the gain constants by dynamic values.
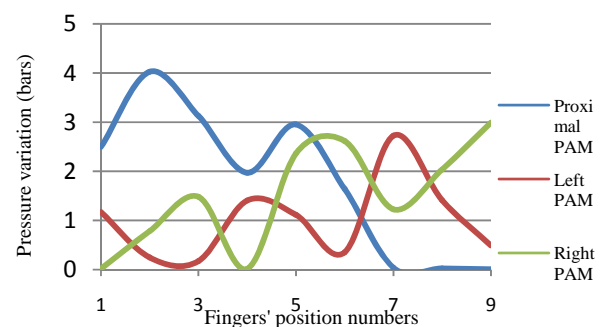

Fig. 2 PAMs' pressure variation according to fingers' extreme positions, where position 1 refers to "proximal and medial / distal phalanges on left side", position 2 refers to "proximal phalange on left side, medial / distal phalanges straight", position 3 refers to "proximal phalange on left side, medial / distal phalanges on right side"… and position 9 refers to "proximal and medial / distal phalanges on right side"

World Academy of Science, Engineering and Technology
International Journal of Mechanical and Mechatronics Engineering
Vol:8, No:5, 2014

B. Switching to Dynamic Coefficients

To prevent ambidextrous fingers from oscillating and make the system unstable, a range of critical angles is defined as $\{\theta_c\}$ around the proximal phalange's vertical position. $\{\theta_c\}$ is delimited by θ_{cl} on the left side and by θ_{cr} on the right side. The aim of the PPSC is to anticipate $\{\theta_c\}$ and to switch the classic gain constants used in (1) into dynamic coefficients. To allow these dynamic coefficients to relay the classic ones before the proximal phalange enters in $\{\theta_c\}$, a danger zone noted $\{\theta_d\}$ is defined as:

$$2\theta_{cl} - \frac{\pi}{2} \le \{\theta_d\} \le 2\theta_{cr} - \frac{\pi}{2} \qquad (2)$$

That allows doubling $\{\theta_c\}$ keeping the proportions around the vertical position. The new limits introduced in (2) are noted θ_{dl} and θ_{dr}. As $\{\theta_d\}$ is defined, the next step consists in calculating appropriate dynamic coefficients to efficiently control the finger around $\{\theta_c\}$. According to the laws of dynamics, an object in motion depends on three parameters: position, velocity and acceleration. For an angle θ, its position is calculated from the equation:

$$\theta(t) = \theta_0 + \omega t - \alpha t^2/2 \qquad (3)$$

with ω its velocity and α its acceleration. As ambidextrous fingers belong to nonlinear systems, their values are estimated from their instantaneous equations, defined as:

$$\omega = \Delta\theta/\Delta t \qquad (4)$$

$$\alpha = \Delta\omega/\Delta t \qquad (5)$$

It is also known that acceleration is obtained from the derivative of speed, itself obtained from the derivative of the position. Consequently, these three values are assimilated to the three terms of the PID controller, based on the error $e(t)$, its integral $\int_0^t e(\tau)d\tau$ and its derivative $\dot{e}(t)$. Based on (2), (3) and (4), the dynamic parameters of the proximal phalange are compared to the following values whenever the finger goes from its left side to a vertical position or to its right side:

$$K_p * e(t) < [\pi/2 - \theta_{dl} + \theta(t)]/\Delta t \qquad (6)$$

$$K_i * \int_0^t e(\tau)d\tau < \pi/2 - \theta(t) \qquad (7)$$

$$K_d * \dot{e}(t) < \left[2K_p e(t)\Delta t - \theta(t)\right] / \Delta^2 t \qquad (8)$$

As soon as the inequality goes wrong either for the position term, or both the velocity and acceleration terms, it is estimated that the proximal phalange is going to reach $\{\theta_c\}$, which triggers the PPSC. The constant gains of the PID are consequently switched to their dynamic values, defined as:

$$K_{dp} = |\pi/2 - \theta(t)| + C_{dp} \qquad (9)$$

$$K_{di} = |(\pi/2 - \theta(t)) * \dot{e}(t)|/(|e(t)| + C_{di}) \qquad (10)$$

$$K_{dd} = \theta(t) * K_{di} /(|e(t)| + C_{dd}) \qquad (11)$$

where C_{dp} is a small positive constant preventing the system to become motionless, whereas C_{di} and C_{dd}, also positive, stabilize the speed and the acceleration for an angle close to $\pi/2$. Contrary to the constant coefficients, the dynamic ones take the angular distance into account as well as the error; they react in different ways depending on if θ_t belongs to $\{\theta_d\}$ or to the finger's right side. In the first case, the motion prepares to slow down as the setpoint is very close, whereas in the second case the speed aims to be constant. An identical method is symmetrically applied when the finger starts from its right position. In both cases, it can be noted that the dynamic coefficients are specific to positions close to vertical and so cannot be used permanently (as the finger motion would be very slow or otherwise irregular) which is why the PPSC is required. Finger positions are shown in Fig. 3, when the Ambidextrous Robot Hand was under construction. However, even though the system stays stable and the positions are very accurate, it is noted that the PPSC can make the finger speed vary when θ_t belongs to $\{\theta_d\}$. Later on, the design was finalized and the parallel abilities of fingers were investigated, mainly concerning its grasping abilities. This is the reason why a system controlling both the angular displacement and the PAMs' pressure is modelled using SMC.

III. CONTROL OF GRASPING ABILITIES

PAMs' pressure is directly related to the force applied by the fingers and, consequently, to its interactions with objects. Because of PAMs' nonlinearity, the algorithm investigated is based on SMC, as it allows to drive a state trajectory (defined as an error) toward a predefined phase plane and to slide along its surface [20]. In the case of ambidextrous fingers, data feedback is continuously analyzed during their motion, both for their angle $\theta(t)$ and their pressure $p(t)$. They are always compared to their precedent values to check if the fingers trajectories present some irregularities. The following inequality is defined for this purpose:

$$\begin{bmatrix} \Delta\theta(t) * K_\pi \Delta p(t) \\ \Delta\dot{\theta}(t) * K_\pi \Delta\dot{p}(t) \end{bmatrix} < \begin{bmatrix} K_{\theta p} \\ K_{\dot{\theta}\dot{p}} \end{bmatrix} \qquad (12)$$

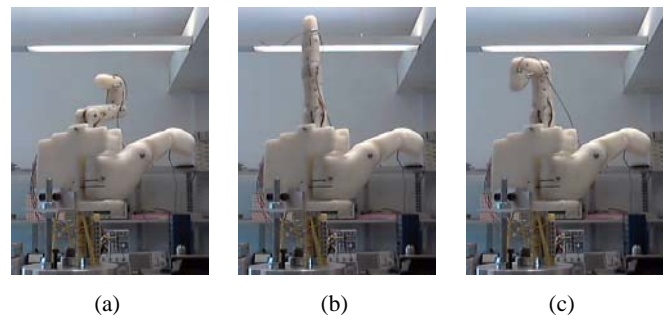|		
(a)	(b)	(c)

Fig. 3 Video snapshots of finger positions obtained with PID loops coupled with a PPSC on an intermediate design of the Ambidextrous Hand. By analogy with Fig. 2, (a) corresponds to position 3, (b) to position 5 and (c) to position 6

World Academy of Science, Engineering and Technology
International Journal of Mechanical and Mechatronics Engineering
Vol:8, No:5, 2014

where,

$$K_\pi = \theta_{Max} / p_{Max} \tag{13}$$

so angles and pressure have an equivalent impact in the inequality. $K_{\theta p}$ and $K_{\theta \dot{p}}$ are constant ratios different for each PAMs and obtained from the experiment shown in Fig. 2. When at least one inequality of (13) goes wrong, it means a phalange is in contact with an object. With a method very similar to the one described in [17], the sliding surface is then defined as:

$$S(t) = K_{\theta p}[\Delta\theta(t) * K_\pi \Delta p(t)] + \Delta\dot{\theta}(t) * K_\pi \Delta\dot{p}(t) \tag{14}$$

$$\dot{S}(t) = K_{\theta p}[\Delta\dot{\theta}(t) * K_\pi \Delta\dot{p}(t)] + \Delta\ddot{\theta}(t) * K_\pi \Delta\ddot{p}(t) \tag{15}$$

with $K_{\theta p}$ calculated as:

$$K_{\theta p} = [\Delta\dot{\theta}(t) * K_\pi \Delta\dot{p}(t)_{Max}] / [\Delta\theta(t) * K_\pi \Delta p(t)]_{Max} \tag{16}$$

Then the convergence to $\{S(t), \dot{S}(t)\}$ is achieved using a Lyapunov function to bring the system to an equilibrium point:

$$L = K_{PAM} * S(t) * \dot{S}(t) \tag{17}$$

In the case of PAM technology, K_{PAM} is usually chosen as ½ such as in [16], [21], but because of the fingers asymmetrical tendon routing, the coefficient attributed to each PAM varies from one to another, as in II.A. Thus, the maximum value of K_{PAM} is defined as ½, but is often reduced according to the phalange position provided by $\theta(t)$. The boundary surface is consequently described as:

$$l = K_{PAM}\dot{S}(t) + \tanh(K_{PAM} * S(t)/\varepsilon_b) \tag{18}$$

So, the phalanges are going to tighten around the object, sliding along the limit defined by the Lyapunov function until:

$$\Delta\theta(t) < \varepsilon_o \tag{19}$$

where ε_o is a small constant, aiming at stopping the SMC when the angle barely varies between two successive feedbacks. The bigger ε_o, the more delicate the object is that the Ambidextrous Hand can grab; the smaller the grabbing force. The efficiency of this method is shown in Fig. 4, where the Ambidextrous Hand is grabbing two fragile objects of different shapes on both sides, for the same ε_o. The structure of the whole control approach is illustrated in Fig. 5.

The experiment illustrated in Fig. 4 (a) is repeated a number of times to collect data. Putting the egg at close initial positions for each run, the final angles reached by the concerned metacarpo-phalangeal joints (MCP) and the proximal interphalangeal joints (PIP) are gathered in Fig. 6. It is seen that MCP and PIP joints depend on each other: when one decreases, the other one increases to secure the grasping. As the new design of the ambidextrous hand stepped aside the thumb opposition in favor of its abduction / adduction, it is

also noted that only the force of the thumb's adduction is applied to the object. Consequently, the objects are not in contact with the inside of the thumb but with its side, which makes the grasping not as human-like as the ones that would be possible, for instance, with the motorized control system introduced in [22]. However, the holding features of the ambidextrous hand are still more anthropomorphic than the ones of the two-fingered and three-fingered motorized robot hands respectively concerned in [23] and [24], even though these two models have other advantages. Indeed, changing the shape of the hand, as well as the position and the number of fingers, can ease the implementation of control algorithms, allowing a stronger grasp and so an accurate manipulation of objects, as shown by the stability of the system described in [25]. Nevertheless, despite its thumb limitation, the experiments proved that the Ambidextrous Hand can grab objects in a similar way to that of the robot hands illustrated in [26].

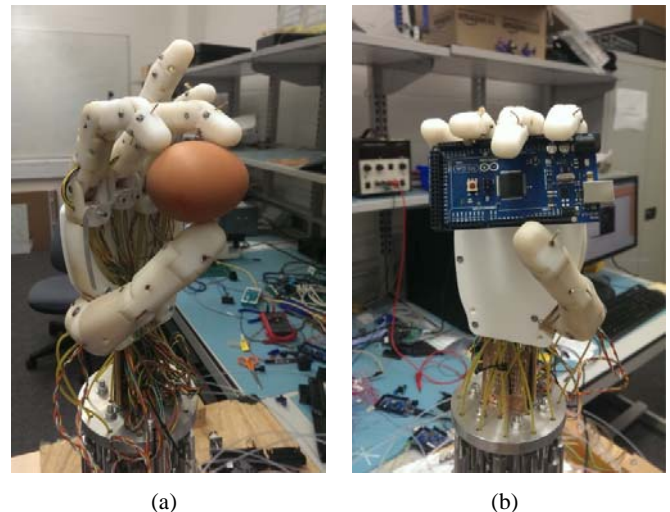(a)   (b)

Fig. 4 Grasping abilities of the Ambidextrous Robot Hand. The left hand mode grabs an egg on (a) whereas the right hand mode grabs an Arduino microcontroller on (b). It is noted that ring and little fingers came back to a position close to vertical on (a), as the angular and pressure feedbacks revealed that they were not in contact with any objects
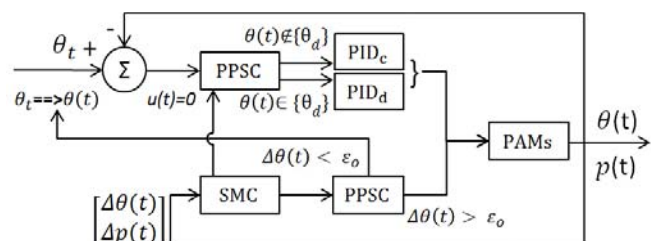

Fig. 5 Global diagram of the described control approach. It is noted that the PID loops are stopped when the SMC is triggered and that the grasping angle is put as the new setpoint when the SMC stops

World Academy of Science, Engineering and Technology
International Journal of Mechanical and Mechatronics Engineering
Vol:8, No:5, 2014

During these same experiments, in addition to joint angles, the pressure of PAMs is also collected. Their grasping values are gathered in Fig. 7. Except the thumb's adduction that is controlled by its right PAM, it is seen for the other joints thatthe higher the pressure, the smaller the angle and that the PAMs connected to the MCP joints require more pressure than PIP's ones. Despite the asymmetrical architecture, it is noted that the ambidextrous fingers are approximately as accurate and as stable as the ones of other models. Indeed, the pressure variation of PAMs is roughly as small as the one of the two muscles robot arm presented in [27] or as the pneumatic assist wear introduced in [28], whereas the angles of the force control mode are very close to the results introduced in [29].

IV. CONCLUSION

A first approach to control the fingers motions and the grasping abilities of a unique ambidextrous hand design was introduced in this paper. The experiments carried out with the robotic device confirmed that the proposed control system is appropriate for both cases, even though the finger motion may vary for a setpoint close to the vertical position. The next steps of the control approach consist in linearizing the angular speed and in increasing the possible interactions with objects, such as moving them up and down or to transfer the force applied from one finger to another.
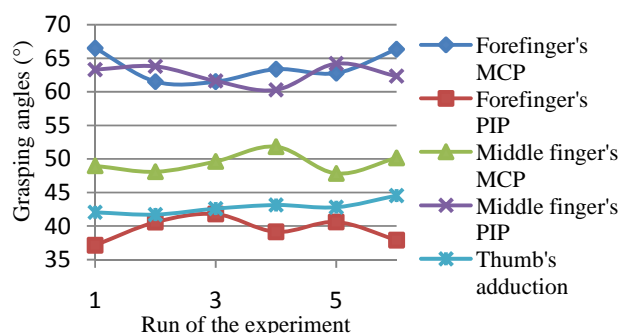

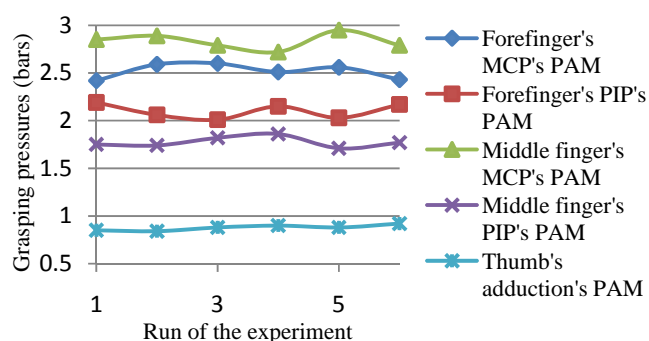Fig. 6 Joints' angles when the ambidextrous hand is holding an egg

Fig. 7 PAMs' pressures when the ambidextrous hand is holding an egg

ACKNOWLEDGMENT

REFERENCES

[1] E. Akyürek, L. Paramonov, L. Steele, M. Simko, L. Kavanagh, A. Nimmo, A. Huynh, Stelarc, and T. Kalganova, " Ambidextrous Design for a Robotic Hand Actuated by Pneumatic Artificial Muscles", unpublished.

[2] A.D. Deshpande, Z. Xu, M.J. Vande Weghe, B.H. Brown, J. Ko, L.Y. Chang, D.D Wilkinson, S.M. Bidic, and Y. Matsuoka, "Mechanisms of the Anatomically Correct Testbed (ACT) Hand", *IEEE/ASME Transactions on Mechatronics,* vol. 18, 2013, pp. 238-250.

[3] Shadow Robot Company Ltd, *Shadow Dexterous Hand E1M3R, E1M3L,* 2013.

[4] A. Ikeda, Y. Kurita, and T. Ogasawara "Evaluation of Pinching Effort by a Tendon-Driven Robot Hand", *Proceedings of 2009 IEEE International Conference on Robotics and Automation (ICRA),* 2009, pp. 3437-3442.

[5] G. Berselli, G. Borghesan, M. Brandi, C. Melchiorri, C. Natale, G. Palli, S. Pirozzi, and G. Vassura, "Integrated Mechatronic design for a new generation of robotic hands", *9th IFAC Symposium on Robot Control,* 2009, pp. 8-13.

[6] D.G. Caldwell, G.A. Medrano-Cerda, and M. Goodwin "Control of Pneumatic Muscle Actuators", *IEEE Control Systems,* 1995, pp. 40-47.

[7] R.V. Ham, B. Verrelst, F. Daerden, and D. Lefeber, "Pressure Control with On-Off Valves of Pleated Pneumatic Artificial Muscles in a Modular One-Dimensional Rotational Joint", *International Conference on Humanoid Robots,*2003,abstract p. 35.

[8] A. Hildebrandt, O. Sawodny, R. Neumann, and A. Hartmann, "A Cascaded Tracking Control Concept for Pneumatic Muscle Actuators", *American Control Conference, 2005. Proceedings of the 2005,* vol. 1, 2005, pp. 680-685.

[9] X. Zhu, G. Tao, B. Yao, and J. Cao, "Adaptive Robust Posture Control of Parallel Manipulator Driven by Pneumatic Muscles with Redundancy", *IEEE/ASME Transactions on Mechatronics,* vol. 13, no. 4, 2008, pp. 441-450.

[10] T.J. Yeh, M.J. Wu, T.J. Lu, F.K. Wu, and C.R. Huang, "Control of McKibben pneumatic muscles for a power-assist, lower-limb orthosis", *Mechatronics,* vol. 20, no. 6, 2010, pp. 686-697.

[11] E. Akyürek, A. Dilly, F. Jourdan, Z. Liu, S. Chattoraj, I. Berruezo Juandeaburre, M. Heinrich, L. Paramonov, P. Turner, Stelarc, and T. Kalganova, "Remote-Controlled Ambidextrous Robot Hand Concept", *Journal of Computer Technology and Application,* vol. 4, no. 4, 2013, pp. 569-574.

[12] K.K. Ahn and N.H. Thai Chau "Intelligent Phase Plane Switching Control of a Pneumatic Muscle Robot Arm with Magneto-Rheological Brake", *Journal of Mechanical Science and Technology,* vol. 21, 2007, pp. 1196-1206.

[13] Z. Tong, Z. Ling, and W. Tao, "New Sliding Mode Control for Pneumatic Muscle Actuator Joint Model via Delta Operator Approach", *Third International Conference on Measuring Technology and Mechatronics Automation (ICMTMA),* vol. 2, 2011, pp. 686-689.

[14] H. Aschemann and D. Schindele, "Sliding-Mode Control of a High-Speed Linear Axis Driven by Pneumatic Muscle Actuators", *IEEE Transactions on Industrial Electronics,* vol. 55, no. 11, 2008, pp. 3855-3864.

[15] M. Chettouh, R. Toumi, and M. Hamerlain, "High-Order Sliding Modes for a Robot Driven by Pneumatic Artificial Rubber Muscles", *Advanced Robotics,* vol. 1, no. 22, 2008, pp. 689-704.

[16] S. Boudoua, F. Hamerlain, and M. Hamerlain, "Neuro Sliding Mode Based Chatter Free Control for an Artificial Muscles Robot Arm",

World Academy of Science, Engineering and Technology
International Journal of Mechanical and Mechatronics Engineering
Vol:8, No:5, 2014

International Joint Conference on Neural Networks (IJCNN), 2010, pp. 1-7.

[17] H. Aschemann and D. Schindele, "Nonlinear Model-Based Control of a Parallel Robot Driven by Pneumatic Muscle Actuators" in *New approaches in Automation and Robotics,* ed. Harald Aschemann, I-Tech Education and Publishing, 2008.

[18] K.H. Ang, G. Chong, and Y. Li "PID Control System Analysis, Design, and Technology", *IEEE Transactions on Control Systems Technology,* vol. 13, no. 4, 2005, pp. 559-576.

[19] Y. Honda, F. Miyazaki and A. Nishikawa, "Control of pneumatic five-fingered robot hand using antagonistic muscle ratio and antagonistic muscle activity", *Proc. 3rd IEEE RAS & EMBS International Conference on Biomedical Robotics and Biomechatronics*, 2010, pp. 337-342.

[20] K.D. Young, V.I. Utkin, and Ü. Özgüner, "A Control Engineer's Guide to Sliding Mode Control", *IEEE Transactions on Control Systems Technology,* vol. 7, no. 3, 1999, pp. 328-342.

[21] M.R. Soltanpour and M.M. Fateh, "Sliding Mode Robust Control of Robot Manipulator in the Task Space by Support of Feedback Linearization and BackStepping Control", *World Applied Sciences Journal,* vol. 6, no. 1, 2009, pp. 70-76.

[22] A.D. Deshpande, J. Ko, D. Fox, and Y. Matsuoka, "Anatomically Correct Testbed Hand Control: Muscle and Joint Control Strategies", *IEEE International Conference on Robotics and Automation*, 2009, pp. 4416-4422.

[23] D. Gunji, Y. Mizoguchi, S. Teshigawara, A. Ming, A. Namiki, M. Ishikawa and, and M. Shimojo, "Grasping Force Control of Multi-Fingered Robot Hand based on Slip Detection Using Tactile Sensor", *IEEE International Conference on Robotics and Automation (ICRA)*, 2008, pp. 2605-2610.

[24] T. Hasegawa, K. Murakami, and T. Matsuoka, "Grasp Planning for Precision Manipulation by Multifingered Robotic Hand", *IEEE International Conference on Systems, Man, and Cybernetics*, 1999, pp. 762-767.

[25] T. Yoshikawa, "Multifingered robot hands: Control for grasping and manipulation", *Annual Reviews in Control*, 2010, pp. 199-208.

[26] M.A. Roa, M.J. Argus, D. Leidner, C. Borst, and G. Hirzinger, "Power Grasp Planning for Anthropomorphic Robot Hands", *IEEE International Conference on Robotics and Automation (ICRA),* 2012, pp. 563-569.

[27] P. Pomiers, "Modular Modular Robot Arm Based on Pneumatic Artificial Rubber Muscles (PARM)", *Proceedings of the 6th International Conference on Climbing and Walking Robots and the Support Technologies for Mobile Machines*, 2003, 879-886.

[28] T. Noritsugu, M. Takaiwa, and D. Sasaki, "Power Assist Wear with Pneumatic Rubber Artificial Muscles", *Mechatronics and Machine Vision in Practice*, 2008, pp. 539-544.

[29] X. Jiang, C. Xiong, R. Sun, and Y. Xiong, "Characteristics of the Robotic Arm of a 9-DoF Upper Limb Rehabilitation Robot Powered by Pneumatic Muscles", *Intelligent Robotics and Applications*, Springer Berlin Heidelberg, 2010, pp 463-474.